World Academy of Science, Engineering and Technology
International Journal of Physical and Mathematical Sciences
Vol:11, No:12, 2017

The Search of Anomalous Higgs Boson Couplings at the Large Hadron Electron Collider and Future Circular Electron Hadron Collider

Ilkay Turk Cakir, Murat Altinli, Zekeriya Uysal, Abdulkadir Senol, Olcay Bolukbasi Yalcinkaya, Ali Yilmaz

***Abstract*—**The Higgs boson was discovered by the ATLAS and CMS experimental groups in 2012 at the Large Hadron Collider (LHC). Production and decay properties of the Higgs boson, Standard Model (SM) couplings, and limits on effective scale of the Higgs boson's couplings with other bosons are investigated at particle colliders. Deviations from SM estimates are parametrized by effective Lagrangian terms to investigate Higgs couplings. This is a model-independent method for describing the new physics. In this study, sensitivity to neutral gauge boson anomalous couplings with the Higgs boson is investigated using the parameters of the Large Hadron electron Collider (LHeC) and the Future Circular electron-hadron Collider (FCC-eh) with a model-independent approach. By using MadGraph5_aMC@NLO multi-purpose event generator with the parameters of LHeC and FCC-eh, the bounds on the anomalous HγγH, HγZ and HZZ couplings in $e^- p \to e^- q H$ process are obtained. Detector simulations are also taken into account in the calculations.

***Keywords*—**Anomalous Couplings, Effective Lagrangian, Electron-Proton Colliders, Higgs Boson.

I. Introduction

THE Higgs boson is discovered at the ATLAS [1] and CMS [2] experiments. Investigating the Higgs boson's interactions with Standard Model (SM) particles is important for the search of the new physics effects beyond the SM. In order to probe the strength and structure of the Higgs boson's interactions, effective field theory approach [3]–[8] can be adopted. In the effective field theory, dimension six or higher operators are added to the SM Lagrangian. Some of these operators produce new tensor structures for the Higgs boson's interactions with SM particles. The effective Lagrangian is shown as:

$$\mathcal{L}_{eff} = \mathcal{L}_{SM} + \sum_i \frac{c_i \mathcal{O}_i}{\Lambda^2}, \tag{1}$$

where $\mathcal{L}_{SM}$ is the SM Lagrangian, c_i are the Wilson coefficients, $\mathcal{O}_i$ are the dimension six operators and Λ is the effective energy scale of the new physics effects.

I. Turk Cakir is with the Giresun University, Department of Energy Systems Engineering, 28200, Giresun, Turkey and CERN, Geneva, Switzerland (e-mail: ilkay.turk.cakir@cern.ch).

Z. Uysal is with Gaziantep University, Department of Engineering Physics, 27310, Gaziantep, Turkey (e-mail: zekeriya.uysal@cern.ch).

A. Senol is with Abant Izzet Baysal University, Department of Physics, 14280, Bolu, Turkey (e-mail: senol_a@ibu.edu.tr).

M. Altinli and O. Bolukbasi Yalcinkaya are with Istanbul University, Department of Physics, 34134, Istanbul, Turkey (e-mail: altinli_murat@hotmail.com, olcayblkba@hotmail.com).

A. Yilmaz is with Giresun University, Department of Electric and Electronics Engineering, 28200, Giresun, Turkey (e-mail: aliyilmaz@giresun.edu.tr).

In this study, the effects of operators that produce anomalous CP-conserving and CP-violating HVV (V = γ, Z) interactions are investigated with an effective Lagrangian using the parameters of Large Hadron electron Collider (LHeC) [9] and Future Circular electron-hadron Collider (FCC-eh) [10].

II. Higgs Effective Lagrangian

The effective Lagrangian for the anomalous HVV interaction is given by [11]:

$$\begin{aligned}\mathcal{L}_{eff} = &-\frac{1}{4} g_{h\gamma\gamma} F_{\mu\nu} F^{\mu\nu} h - \frac{1}{4} \tilde{g}_{h\gamma\gamma} F_{\mu\nu} \tilde{F}^{\mu\nu} h \\ &- \frac{1}{4} g^{(1)}_{hzz} Z_{\mu\nu} Z^{\mu\nu} h - g^{(2)}_{hzz} Z_\nu \partial_\mu Z^{\mu\nu} h \\ &+ \frac{1}{2} g^{(3)}_{hzz} Z_\mu Z^\mu h - \frac{1}{4} \tilde{g}_{hzz} Z_{\mu\nu} \tilde{Z}^{\mu\nu} h \\ &- \frac{1}{2} g^{(1)}_{haz} Z_{\mu\nu} F^{\mu\nu} h - \frac{1}{2} \tilde{g}_{haz} Z_{\mu\nu} \tilde{F}^{\mu\nu} h \\ &- g^{(2)}_{haz} Z_\nu \partial_\mu F^{\mu\nu} h.\end{aligned} \tag{2}$$

Here $g_{h\gamma\gamma}$, $g^{(1)}_{hzz}$, $g^{(2)}_{hzz}$, $g^{(3)}_{hzz}$, $g^{(1)}_{haz}$ and $g^{(2)}_{haz}$ couplings are CP-conserving whereas $\tilde{g}_{h\gamma\gamma}$, $\tilde{g}_{hzz}$ and $\tilde{g}_{haz}$ are CP-violating. The $g_{h\gamma\gamma}$ and $\tilde{g}_{h\gamma\gamma}$ couplings contain only $\bar{c}_\gamma$ and $\tilde{c}_\gamma$ coefficients, respectively; the $g^{(1)}_{hzz}$ and $g^{(1)}_{haz}$ couplings contain $\bar{c}_{HW}$, $\bar{c}_{HB}$ and $\bar{c}_\gamma$ coefficients; the $\tilde{g}_{hzz}$ and $\tilde{g}_{haz}$ couplings contain $\tilde{c}_{HW}$, $\tilde{c}_{HB}$ and $\tilde{c}_\gamma$ coefficients; the $g^{(2)}_{hzz}$ and $g^{(2)}_{haz}$ couplings contain $\bar{c}_{HW}$, $\bar{c}_{HB}$, $\bar{c}_W$ and $\bar{c}_B$ coefficients, and the $g^{(3)}_{hzz}$ coupling contains $\bar{c}_H$, $\bar{c}_T$ and $\bar{c}_\gamma$ coefficients. The coupling constants appearing in the effective Lagrangian are given in Table I with their relation to the Wilson coefficients.

TABLE I
Coupling Constants of the Interactions of a Higgs Boson with a Vector Boson Pair

$g_{h\gamma\gamma}$	$a_H - \frac{8g\bar{c}_\gamma s_W^2}{m_W}$
$\tilde{g}_{h\gamma\gamma}$	$-\frac{8g\tilde{c}_\gamma s_W^2}{m_W}$
$g^{(1)}_{hzz}$	$\frac{2g}{c_W^2 m_W}\left[\bar{c}_{HB} s_W^2 - 4\bar{c}_\gamma s_W^4 + c_W^2 \bar{c}_{HW}\right]$
$\tilde{g}_{hzz}$	$\frac{2g}{c_W^2 m_W}\left[\tilde{c}_{HB} s_W^2 - 4\tilde{c}_\gamma s_W^4 + c_W^2 \tilde{c}_{HW}\right]$
$g^{(2)}_{hzz}$	$\frac{2g}{c_W^2 m_W}\left[\left(\bar{c}_{HW} + \bar{c}_W\right) c_W^2 + \left(\bar{c}_B + \bar{c}_{HB}\right) s_W^2\right]$
$g^{(3)}_{hzz}$	$\frac{g m_W}{c_W^2}\left[1 - \frac{1}{2}\bar{c}_H - 2\bar{c}_T + 8\bar{c}_\gamma \frac{s_W^4}{c_W^2}\right]$
$g^{(1)}_{haz}$	$\frac{g s_W}{c_W m_W}\left[\bar{c}_{HW} - \bar{c}_{HB} + 8\bar{c}_\gamma s_W^2\right]$
$\tilde{g}_{haz}$	$\frac{g s_W}{c_W m_W}\left[\tilde{c}_{HW} - \tilde{c}_{HB} + 8\tilde{c}_\gamma s_W^2\right]$
$g^{(2)}_{haz}$	$\frac{g s_W}{c_W m_W}\left[\bar{c}_{HW} - \bar{c}_{HB} - \bar{c}_B + \bar{c}_W\right]$

In this study, Wilson coefficients are varied in the range [-0.1, 0.1] and the cross sections are calculated for $e^- p \to e^- q\, H$ process. Tree level Feynman diagrams that include H$\gamma\gamma$, HγZ and HZZ couplings for this process are given in Fig. 1.

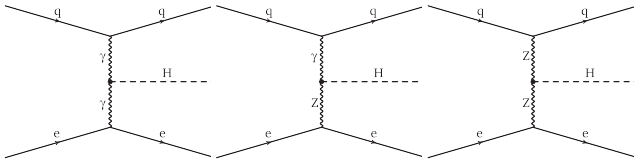

Fig. 1 Feynman diagrams for $e^- p \to e^- q\, H$ process that include HVV vertices

III. The Cross Sections

In this study, MadGraph5_aMC@NLO (v2.3.3) [12] program is used to generate the events for the given processes. Since effective field theory approach is adopted, HEL_UFO [11], [13] model file implemented through FeynRules [14] is used instead of default SM model file. The energy parameters of both LHeC and FCC-eh are used for all the events generated for the signal and background processes. LHeC has 60 GeV electron and 7 TeV proton beams while FCC-eh has 60 GeV electron and 50 TeV proton beams. Pythia (v6.428) [15] is used for the hadronisation and decay of the produced jets in the generated events. The interaction of the generated particles with the detector, and its response, are simulated using Delphes (v3.3.0) [16]. ATLAS and FCC detector cards are used for LHeC and FCC-eh, respectively.

A. Signal Cross Sections

The cross section of the $e^- p \to e^- q\, H$ signal process is calculated for Wilson coefficient values between -0.1 and 0.1. The Wilson coefficients used in this calculation are $\bar{c}_\gamma$, $\bar{c}_{HW}$, $\bar{c}_{HB}$, $\bar{c}_W$, $\bar{c}_B$, $\bar{c}_H$, $\bar{c}_T$, $\tilde{c}_\gamma$, $\tilde{c}_{HW}$ and $\tilde{c}_{HB}$. Each one of these coefficients are taken into account individually, meaning that while one is varied between -0.1 and 0.1, the others are set to zero. The plot for cross sections according to the CP-even coefficient values at LHeC and FCC-eh are given in Fig. 2 and 3, respectively.

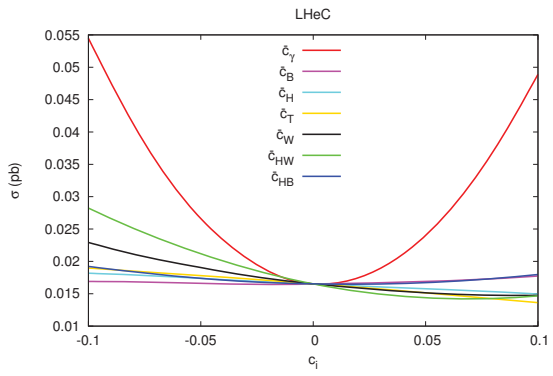

Fig. 2 Cross sections for CP-even coefficient values at LHeC

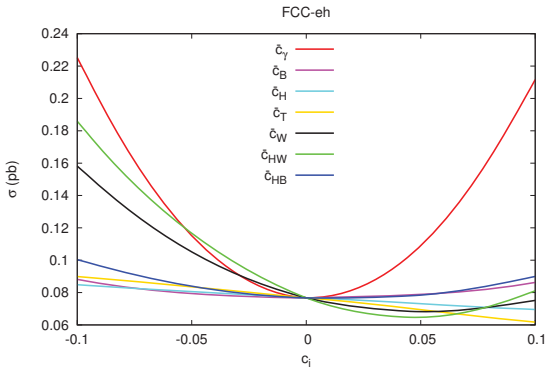

Fig. 3 Cross sections for CP-even coefficient values at FCC-eh

The cross section plots for the CP-odd coefficients are shown in Fig. 4 and 5, at LHeC and FCC-eh, respectively.

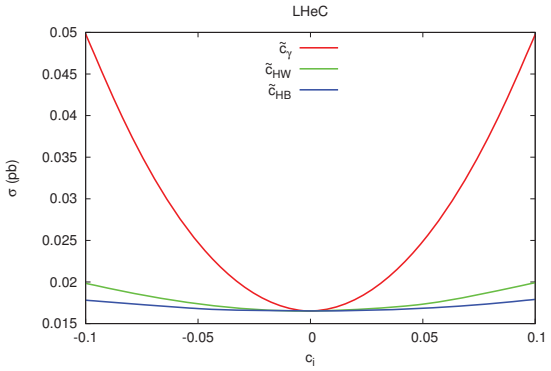

Fig. 4 Cross sections for CP-odd coefficient values at LHeC

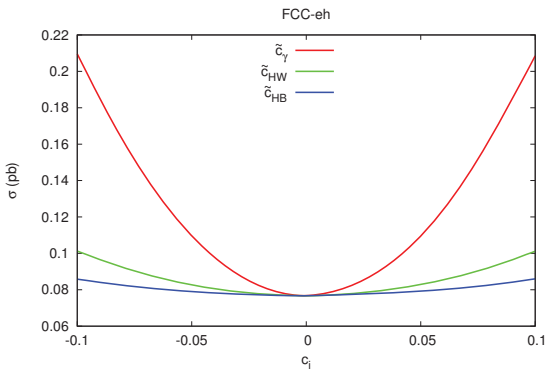

Fig. 5 Cross sections for CP-odd coefficient values at FCC-eh

B. Cross Sections for the Signal with Polarised Electron

Here, the cross section calculations are made by taking into account 80% left-handed polarisation of the incident electron in the $e^- p \to e^- q\, H$ process while the Wilson coefficients are individually varied between -0.1 and 0.1. The plots of the

cross sections dependent on CP-even coefficients at LHeC and FCC-eh are given in Fig. 6 and 7, respectively.

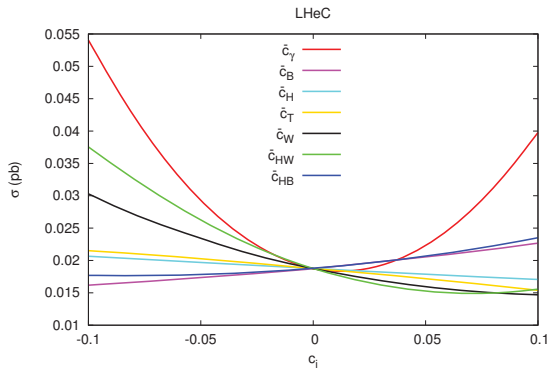

Fig. 6 Cross sections for CP-even coefficient values with polarised electron at LHeC

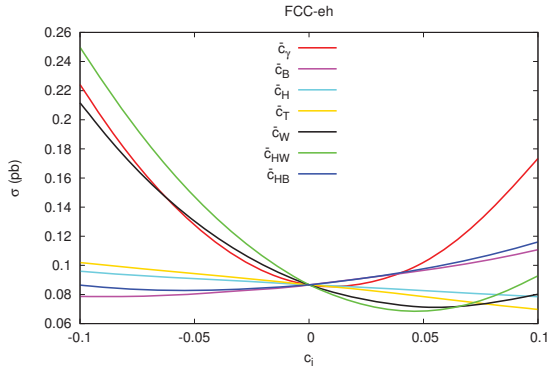

Fig. 7 Cross sections for CP-even coefficient values with polarised electron at FCC-eh

The cross section plots for CP-odd coefficients are shown in Fig. 8 and 9, at LHeC and FCC-eh, respectively.

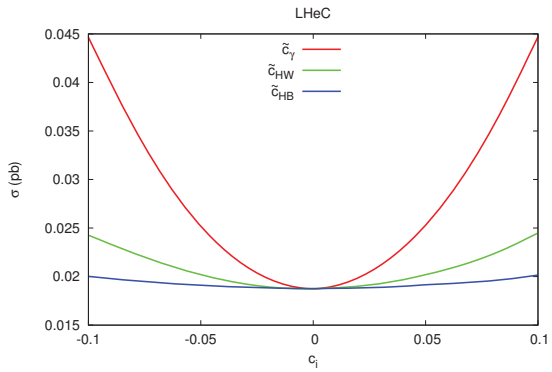

Fig. 8 Cross sections for CP-odd coefficient values with polarised electron at LHeC

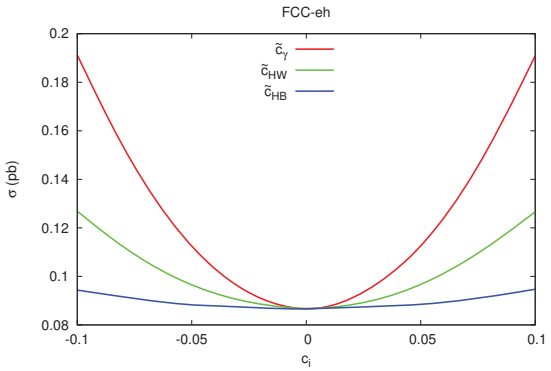

Fig. 9 Cross sections for CP-odd coefficient values with polarised electron at FCC-eh

C. Background Cross Sections

Five background processes are taken into account for the cross section calculation. These are $e^-p \rightarrow e^-q\,H$, $e^-p \rightarrow e^-q\,Z$, $e^-p \rightarrow e^-q\,W^{\pm}$, $e^-p \rightarrow e^-W^{\pm}t(\bar{t})$ and $e^-p \rightarrow e^-t\,\bar{t}$ processes. Cross sections of these background processes with and without electron polarisation are shown in Table II.

TABLE II
BACKGROUND CROSS SECTIONS AT LHEC AND FCC-EH WITH AND WITHOUT ELECTRON POLARISATION (80% LEFT-HANDED)

Background process	Cross sections (pb)			
	No polarisation		Electron polarisation	
	LHeC	FCC-eh	LHeC	FCC-eh
$e^-p \rightarrow e^-q\,H$	0.017	0.077	0.0187	0.0865
$e^-p \rightarrow e^-q\,Z$	0.203	0.625	0.2631	0.8095
$e^-p \rightarrow e^-q\,W^{\pm}$	2.305	8.654	3.169	12.14
$e^-p \rightarrow e^-W^{\pm}t(\bar{t})$	0.011	0.229	0.0148	0.3138
$e^-p \rightarrow e^-t\,\bar{t}$	0.015	0.417	0.0171	0.467

IV. Analysis

In this section, the analysis of the results obtained from the detector simulation is shown. For the analysis, the invariant mass of the Higgs boson is reconstructed by using the invariant mass of two b-tagged jets. Kinematic distributions for the jets and the electron in the signal and background processes are also obtained. For the signal process used in the analysis, $\bar{c}_{HW}$ is equal to -0.03 while all other Wilson coefficients are zero. 80% left-handed polarisation of the electron is taken into account for all the processes.

Transverse momentum and pseudorapidity distributions for the jets and electron are given in Fig. 10 and 11, for the processes with unpolarised and polarised electron, respectively. Only the events that include only one electron and at least three jets are filled into the histograms. Two of the three jets are b-tagged and for the distributions of jets, three jets are filled into the same histogram. Kinematic distributions for all processes, one signal and five background, are shown in separate histograms. Events are normalised for an integrated luminosity of 1 ab^{-1}.

The reconstructed Higgs boson invariant mass is shown in two separate histograms. One is for the signal and

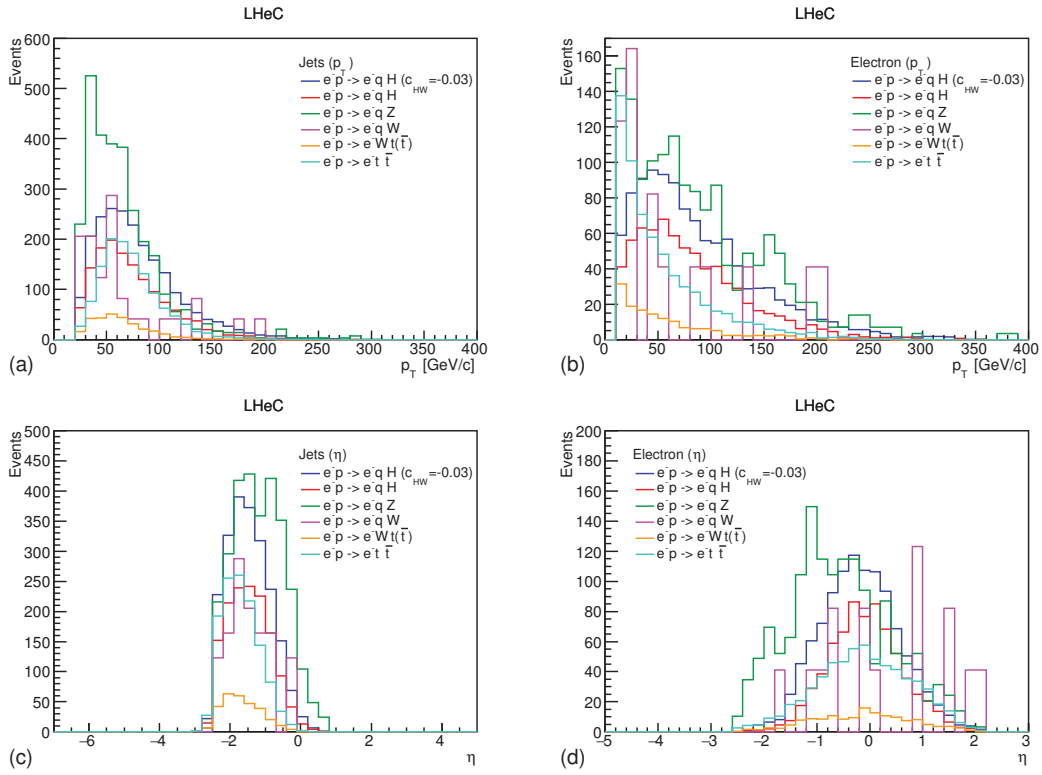

Fig. 10 Transverse momentum (p_T) distributions for (a) jets and (b) electron , and pseudorapidity (η) distributions for (c) jets and (d) electron for the signal and background processes at LHeC ($\Delta R_{bb} < 2$, $L_{int} = 1\ ab^{-1}$)

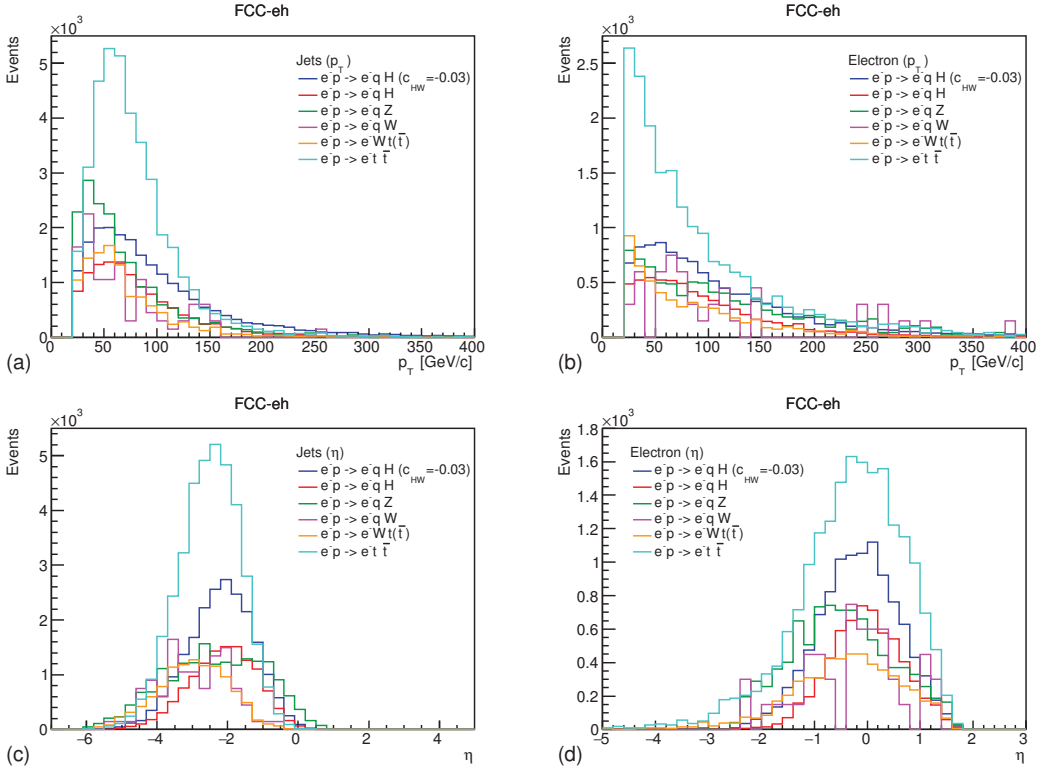

Fig. 11 Transverse momentum (p_T) distributions for (a) jets and (b) electron , and pseudorapidity (η) distributions for (c) jets and (d) electron for the signal and background processes at FCC-eh ($\Delta R_{bb} < 2$, $L_{int} = 1\ ab^{-1}$)

backgrounds, and the other one is only for the backgrounds. Invariant mass distributions are shown in Fig. 12 and 13, at LHeC and FCC-eh, respectively. Events are normalised for $1\ ab^{-1}$ integrated luminosity. Kinematic cuts are applied for jets and electron:

- electron pseudorapidity: $|\eta_e| < 2$,
- pseudorapidity of jets: $-4.5 < \eta_j < 0$,
- transverse momentum of jets: $p_T > 60\,GeV$,
- deltaR of two b-tagged jets: $\Delta R_{bb} < 2$.

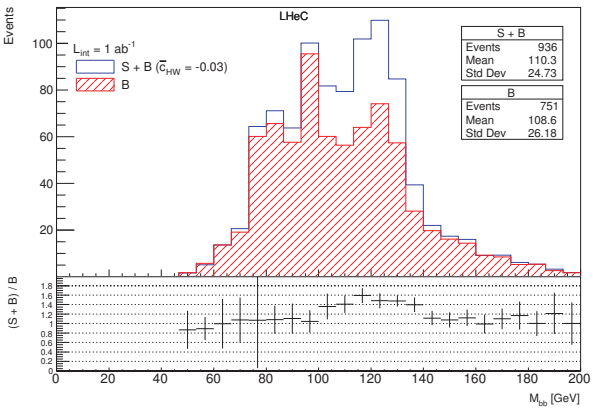

Fig. 12 Invariant mass of two b-tagged jets for signal and background with polarised electron at LHeC

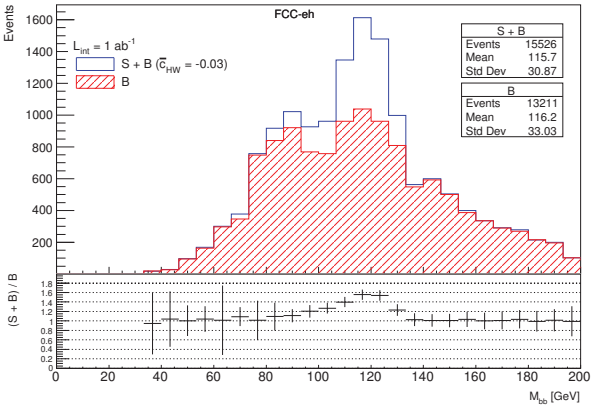

Fig. 13 Invariant mass of two b-tagged jets for signal and background with polarised electron at FCC-eh

V. Statistical Significance

In order to see their sensitivity to the Wilson coefficients, statistical significance (SS) is calculated for both LHeC and FCC-eh using this formula:

$$SS = \sqrt{2[(S+B)\ln\left(1+\frac{S}{B}\right) - S]}. \qquad (3)$$

Here S and B are signal and background event numbers, respectively. For the background event number, all the background processes are taken into account. The decay of the Higgs boson into two b quarks is assumed for the event number calculation. The b-tagging efficiencies are taken to be 60% and 75% for LHeC and FCC-eh, respectively. The integrated luminosity is assumed to be $1ab^{-1}$for both colliders.

The SS values at LHeC and FCC-eh are shown in Fig. 14, while each Wilson coefficient is equal to -0.05 individually. In Fig. 15 where the SS values are shown, each Wilson coefficient is equal to 0.05 individually. Since there is not a significant signal while $\bar{c}_{HW}$, $\bar{c}_W$, $\bar{c}_H$ and $\bar{c}_T$ coefficients have positive values, the SS values for these coefficients do not appear in Fig. 15. In Fig. 14 and 15, there are no polarisation effects.

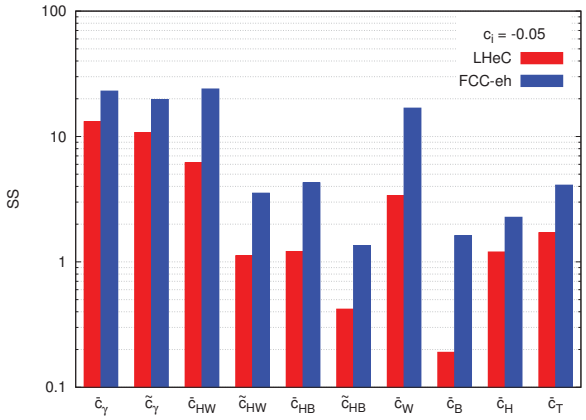

Fig. 14 SS values for Wilson coefficients while their value are -0.05 individually

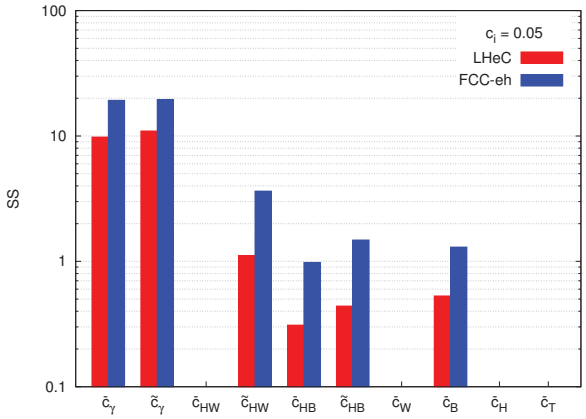

Fig. 15 SS values for Wilson coefficients while their value are 0.05 individually

By using the SS values limits are obtained for each coefficient. The Wilson coefficients are constrained using 2σ significance for the processes with and without electron polarisation at LHeC and FCC-eh. Obtained limits for the Wilson coefficients are given in Table III where they are compared with the limits obtained from LHC Run 1.

TABLE III
LIMITS OBTAINED FOR THE WILSON COEFFICIENTS AT LHEC AND FCC-EH COMPARED TO THE LIMITS OBTAINED FROM LHC RUN 1 [17] (* [18])

Coefficients	LHeC ($1\ ab^{-1}$)		FCC-eh ($1\ ab^{-1}$)		LHC Run 1
	no polarisation	polarisation	no polarisation	polarisation	
$\bar{c}_\gamma$	[-0.015, 0.023]	[-0.015, 0.04]	[-0.011, 0.015]	[-0.01, 0.032]	[−0.00055, 0.00036]
$\bar{c}_B$	[< -0.1,> 0.1]	[< -0.1, 0.048]	[-0.056, 0.063]	[< -0.1, 0.02]	-
$\bar{c}_{HB}$	[-0.07,> 0.1]	[< -0.1, 0.046]	[-0.03, 0.06]	[< -0.1, 0.021]	[−0.086, 0.092]*
$\bar{c}_H$	[-0.088,> 0.1]	[-0.088,> 0.1]	[-0.044,> 0.1]	[-0.044,> 0.1]	[< -0.05, > 0.05]
$\bar{c}_{HW}$	[-0.019,> 0.1]	[-0.014,> 0.1]	[-0.0057,> 0.1]	[-0.0042,> 0.1]	[−0.047, 0.014]
$\bar{c}_T$	[-0.059,> 0.1]	[-0.055,> 0.1]	[-0.024,> 0.1]	[-0.023,> 0.1]	-
$\bar{c}_W$	[-0.033,> 0.1]	[-0.022,> 0.1]	[-0.008,> 0.1]	[-0.0063,> 0.1]	[< -0.01, 0.007]
$\tilde{c}_\gamma$	[-0.021, 0.021]	[-0.026, 0.025]	[-0.016, 0.014]	[-0.019, 0.019]	[-0.0018, 0.0018]
$\tilde{c}_{HB}$	[< -0.1,> 0.1]	[< -0.1,> 0.1]	[-0.061, 0.058]	[-0.07, 0.069]	[-0.23, 0.23]*
$\tilde{c}_{HW}$	[-0.066, 0.066]	[-0.055, 0.055]	[-0.038, 0.036]	[-0.03, 0.031]	[-0.23, 0.23]*

VI. CONCLUSION

The Higgs boson's couplings with γ and Z bosons are investigated using an effective Lagrangian. The limits on Wilson coefficients associated with Higgs boson's couplings are obtained using $e^- p \to e^- q\, H$ signal process at LHeC and FCC-eh. FCC-eh seems to have more potential than LHeC in probing the anomalous Higgs couplings due to its higher center-of-mass energy. By taking into account 80% left-handed polarisation of the electron better limits are obtained for negative values of $\bar{c}_{HW}$, $\bar{c}_W$, positive values of $\bar{c}_{HB}$, $\bar{c}_B$ and both positive and negative values of $\tilde{c}_{HW}$ coefficients.

The results show that the electron-proton colliders have a potential to investigate the anomalous Higgs boson couplings and their sensitivity can be improved for couplings involving weak interactions due to the electron polarisation possibility.

REFERENCES

[1] G. Aad *et al.*, "Observation of a new particle in the search for the Standard Model Higgs boson with the ATLAS detector at the LHC," *Phys. Lett.*, vol. B716, pp. 1–29, 2012.
[2] S. Chatrchyan *et al.*, "Observation of a new boson at a mass of 125 GeV with the CMS experiment at the LHC," *Phys. Lett.*, vol. B716, pp. 30–61, 2012.
[3] J. R. Andersen *et al.*, "Handbook of LHC Higgs Cross Sections: 3. Higgs Properties," 2013.
[4] W. Buchmuller and D. Wyler, "Effective Lagrangian Analysis of New Interactions and Flavor Conservation," *Nucl. Phys.*, vol. B268, pp. 621–653, 1986.
[5] K. Hagiwara, R. Szalapski, and D. Zeppenfeld, "Anomalous Higgs boson production and decay," *Phys. Lett.*, vol. B318, pp. 155–162, 1993.
[6] G. F. Giudice, C. Grojean, A. Pomarol, and R. Rattazzi, "The Strongly-Interacting Light Higgs," *JHEP*, vol. 06, p. 045, 2007.
[7] B. Grzadkowski, M. Iskrzynski, M. Misiak, and J. Rosiek, "Dimension-Six Terms in the Standard Model Lagrangian," *JHEP*, vol. 10, p. 085, 2010.
[8] R. Contino, M. Ghezzi, C. Grojean, M. Muhlleitner, and M. Spira, "Effective Lagrangian for a light Higgs-like scalar," *JHEP*, vol. 07, p. 035, 2013.
[9] J. L. Abelleira Fernandez *et al.*, "A Large Hadron Electron Collider at CERN: Report on the Physics and Design Concepts for Machine and Detector," *J. Phys.*, vol. G39, p. 075001, 2012.
[10] O. Bruning, J. Jowett, M. Klein, D. Pellegrini, D. Schulte, and F. Zimmermann, "Future Circular Collider Study FCC-he Baseline Parameters," Tech. Rep. CERN-ACC-2017-0019, CERN, Geneva, Apr 2017.
[11] A. Alloul, B. Fuks, and V. Sanz, "Phenomenology of the Higgs Effective Lagrangian via FEYNRULES," *JHEP*, vol. 04, p. 110, 2014.
[12] J. Alwall, R. Frederix, S. Frixione, V. Hirschi, F. Maltoni, O. Mattelaer, H. S. Shao, T. Stelzer, P. Torrielli, and M. Zaro, "The automated computation of tree-level and next-to-leading order differential cross sections, and their matching to parton shower simulations," *JHEP*, vol. 07, p. 079, 2014.
[13] C. Degrande, C. Duhr, B. Fuks, D. Grellscheid, O. Mattelaer, and T. Reiter, "UFO - The Universal FeynRules Output," *Comput. Phys. Commun.*, vol. 183, pp. 1201–1214, 2012.
[14] A. Alloul, N. D. Christensen, C. Degrande, C. Duhr, and B. Fuks, "FeynRules 2.0 - A complete toolbox for tree-level phenomenology," *Comput. Phys. Commun.*, vol. 185, pp. 2250–2300, 2014.
[15] T. Sjostrand, S. Mrenna, and P. Z. Skands, "PYTHIA 6.4 Physics and Manual," *JHEP*, vol. 05, p. 026, 2006.
[16] M. Selvaggi, "DELPHES 3: A modular framework for fast-simulation of generic collider experiments," *J. Phys. Conf. Ser.*, vol. 523, p. 012033, 2014.
[17] C. Englert, R. Kogler, H. Schulz, and M. Spannowsky, "Higgs coupling measurements at the LHC," *Eur. Phys. J.*, vol. C76, no. 7, p. 393, 2016.
[18] G. Aad *et al.*, "Constraints on non-Standard Model Higgs boson interactions in an effective Lagrangian using differential cross sections measured in the $H \to \gamma\gamma$ decay channel at $\sqrt{s} = 8$TeV with the ATLAS detector," *Phys. Lett.*, vol. B753, pp. 69–85, 2016.